Environmental conditions during the reported charging anomalies of the two geosynchronous satellites: Telstar 401 and Galaxy 15

E. Saiz[1], C. Cid[1], and A. Guerrero[1]

[1]Space Weather Research Group. Departamento de Física y Matemáticas, Universidad de Alcalá, Alcalá de Henares, Spain.

Corresponding author: Elena Saiz (elena.saiz@uah.es)

Key Points:

- Each anomaly took place during the expansion phase of a triggered substorm, about 45 minutes after a dipolarization
- The interaction between a coronal mass ejection and a high-speed stream appears as the trigger of the substorm that occurred before each anomaly
- The Kp index is not recommended to characterize spacecraft-charging hazards

This article has been accepted for publication and undergone full peer review but has not been through the copyediting, typesetting, pagination and proofreading process which may lead to differences between this version and the Version of Record. Please cite this article as doi: 10.1029/2018SW001974

Abstract

Charging and subsequent Electro Static Discharge (ESD) is recognized as a serious operational threat to spacecraft. This paper concentrates on an analysis of the environmental conditions (geomagnetic measurables, but not the particle fluxes, that were associated with the geomagnetic disturbances) and the interplanetary signatures prior to the anomalies that affected the two geostationary satellites Telstar 401 and Galaxy 15, which were believed to have been caused by spacecraft charging/ESD. In terms of geomagnetic conditions, the planetary Kp index was very different around the two events, despite Kp commonly being used to characterize periods that are hazardous for spacecraft charging. On the contrary, local geomagnetic records, both from GOES satellites and from ground records, reveal that each anomaly took place during the expansion phase of a triggered substorm. Combined with a large and South directed IMF Bz, northward turnings of negative IMF Bz and large fluctuations in IMF By played major roles in the magnetospheric responses of the substorms. The interplanetary features of the two events were also similar: the interplanetary counterpart of coronal mass ejections interacted with high-speed streams, favoring the substorm triggers. Although there are several differences in the preconditioning and the inner conditions of the magnetosphere before the anomalies, in each case the respective spacecraft crossed the plasma sheet in the magnetotail during enhanced substorm activity, with a dipolarization event that took place close to the spacecraft location, indicating that each satellite was in the wrong place at a critical moment.

1 Introduction

The local environment where spacecraft operate greatly affects satellite reliability; even more when this environment is modified due to solar activity. The impact of space weather on the satellite industry is nowadays well known by satellite industry stakeholders and solutions to manage and mitigating impacts are being proposed (Green et al, 2017). Manufacturers are well aware of anomalies due to single event upsets, burnouts and/or latch-ups from energetic protons (>5 MeV); but there are other spacecraft anomalies that can be attributed to the environment, affected by space weather (see, e.g., Farthing et al., 1982; Wilkinson, 1994; Vampola, 1994). Moderately energetic electrons (< 100 keV) can be deposited on spacecraft surfaces and pose a risk of an electrostatic discharge (ESD). Electrons at energies greater than 100 keV can penetrate typical spacecraft structures causing deep dielectric charging, which poses a threat of electrostatic discharge (Iucci et al., 2005; Anderson, 2012). Koons et al. (1998) provided a comprehensive assessment of public space weather anomalies that occurred from 1970 to 1999 and concluded that most anomalies were attributed to ESD. Garrett & Whittlesey (2000) conclude, after the analysis of spacecraft charging over 20 years, that surface charging continues to be recognized as a serious operational threat to spacecraft.

Choi et al. (2011) investigated the Geostationary Earth Orbit (GEO) satellite anomalies archived by Satellite News Digest during 1997-2009 to search for possible influences of space weather on the anomaly occurrences. For that purpose, the Kp index was considered as a proxy for geomagnetic activity and associated with the injection of multi-keV particles from Earth's magnetotail. While Choi et al. (2011) did not explain how space weather is involved in producing such anomalies they concluded that spacecraft charging might dominantly contribute to those spacecraft anomalies. In April 2010 the Galaxy 15 satellite experienced a serious anomaly that disrupted its operation for several months, this was believed to have been caused by an ESD event related to the passage of a magnetic cloud (Loto´aniu et al., 2015; Ferguson et al., 2011; Clilverd et al., 2012); however the solar activity triggering the magnetic cloud cannot be classified as an extraordinary space weather

event. The Kp index was also used by O´Brien (2009) to introduce a spacecraft environmental anomalies expert system for geosynchronous orbit. The system introduces the term 'hazard quotient' defined to quantify the ratio of the instantaneous to mission-averaged likelihood of an anomaly due to each hazard, based on environmental measurements. The ESD hazard quotient peaks in the 4-6 range in the 0-6 MLT sector. This local time range is also pointed out by others authors as the sector where largest signals occurring in electrostatic charge sensors (Ozkul et al., 2001) or where the occurrence frequency of low-energy electron fluxes peaks (Thomsen et al., 2013). These facts might have guided us to state that, quoting to Allen (2010), Galaxy 15 was 'another satellite in the wrong place at a critical time'.

The purpose of this paper is to discuss the criticality of the very specific environmental conditions in terms of time and location to ESD anomalies, and to assess the relevance of more global indices such as Kp. To reach that goal, ESD historical records like Galaxy 15 anomaly should be analyzed. Information about the time and place of the anomaly will be essential for the study. The report by Koons et al. (1998) reviews spacecraft anomalies with a lot of information including the anomaly class, the diagnosis, a description of the impact, and relevant comments and references. However, interplanetary upstream solar wind data are also needed for a proper analysis of the space weather role in these ESD events. Then, only anomalies occurred after 1995, when Wind or Advanced Composition Explorer (ACE) spacecraft data are available, should be considered and this fact excludes all the events reported in Koons et al. (1998). The list included in Table 1 of Choi et al. (2011) is the only source of information known by the authors meeting all three necessary records for the study: the place and the time of the anomaly, a description of the event, and solar wind data available. Only one GEO satellite anomaly appears in the list attributed to ESD: Telstar 401 satellite. The Telstar 401 failure resulting in total loss on 11 January 1997 was previously traced to an ESD due to a space weather event associated with the passage of a magnetic cloud (Lanzerotti et al., 1998b).

This paper compares the environmental conditions and the interplanetary signatures prior to the charging anomalies of the two geostationary satellites reported: Telstar 401 and Galaxy 15. The objective is to find out what common (if any) space weather features made these events so extraordinary as to generate environmental condition conducive to ESD and to explain if the time and place of the spacecraft were relevant for the anomaly. To discuss whether the ESD was the cause of the failures of the spacecraft or it was just a mere coincidence in time is beyond the scope of this paper.

Section 2 presents an overview of the times of the anomalies and respective spacecraft locations and of the available geospace data sources. Section 3 compares both cases describing the geomagnetic conditions at the times of the anomalies, and in Section 4 we analyze interplanetary data and what can be associated with those magnetic conditions. Section 5 evaluates the relevance of the interplanetary and geomagnetic signatures nearby to the anomalies in the operational history of each spacecraft. Section 6 summarizes the results and provides an assessment of the key findings relative to future directions.

2 The Local Time of the Anomalies and the Environmental Data Sources

On 5 April 2010 at 09:48 UT (Universal Time), the geostationary satellite located at 133º geographic West longitude, Galaxy 15, stopped responding to ground commands but did not stop broadcasting signals from its transponders (Allen, 2010). The anomaly occurred while the spacecraft was near local midnight at 01 MLT. The Galaxy 15 anomaly (GA) occurred during multispacecraft observations that included the Geostationary Operational

Environmental Satellite (GOES) 11 to 15, the Time History of Events and Macroscale Interactions during Substorms (THEMIS) probes and the Geotail spacecraft. At that time, GOES 11 (135º W) was located only 2º away in longitude from Galaxy 15. Other GOES spacecraft were at least 30º away in longitude. Geotail was located sunward of the Earth, close to noon. Left panel in Figure 1 shows these spacecraft locations for the time of the GA.

Total loss of Telstar 401 geostationary satellite, located at 97º geographic West longitude, occurred at 11:15 UT on 11 January 1997. The Telstar 401 anomaly (TA) happened while the spacecraft was near local dawn (04:47 MLT). Spacecraft observations during the anomaly come from the GOES 8 and 9, the Los Alamos National Laboratory (LANL) 90 to 91 and 94 and the Geotail spacecraft. The right panel in Figure 1 shows these spacecraft locations for the time of the TA. The closest spacecraft to Telstar 401 during the anomaly was GOES 8, which was more than 20º away in longitude eastwards. LANL 89, also on orbit and close to midnight location at that time, was the spacecraft from the LANL constellation closest to Telstar 401 (almost 50º away in longitude westwards), but on January 11 there is a data gap until 15 UT and therefore data from LANL 89 are not available for this analysis. The other LANL spacecraft were sunward of the Earth at the time of the TA.

3 Geomagnetic Conditions at the Time of the Anomalies

Geomagnetic conditions during a spacecraft anomaly are commonly quantified by the 3-hourly planetary Kp index, ranging in 28 steps from 0 (quiet) to 9 (greatly disturbed). According to the official Kp index web page (https://www.gfz-potsdam.de/en/kp-index/) at the German Research Centre for Geosciences (GFZ), Kp reached 8^- on the interval 09 - 12 UT on 5 April 2010, i.e. during the GA. The planetary daily character (C9), according to the same source, was 7 in a scale between 0 and 9. Previous two days C9 was 3 (April 4) and 2 (April 3), both corresponding to quiet time. The extreme values for geomagnetic activity during the GA are not comparable to those during the TA. On 11 January 1997, the Kp index only reached 4 in the interval 09 - 12 UT and the planetary daily character was 5. Previous two days C9 was 6 (January 10) and 1 (January 9), indicating that the magnetosphere was already disturbed the day before the anomaly.

3.1 Geomagnetic Conditions from GOES Observations

Far from the planetary information provided by Kp, satellite probes, when in proper position, provide measurements of the magnetic environment close to the spacecraft. That is the case during the GA: GOES 11 (only 2º away in longitude from Galaxy 15) was in an excellent location to observe magnetic conditions like those at Galaxy 15. A detailed analysis of magnetic field and particle conditions during GA, including not only GOES 11 observations (extremely close to Galaxy 15) but also GOES 12 to 15 and THEMIS satellite probes was performed by Loto´aniu et al. (2015). Their description of the environment includes a massive magnetic field dipolarization that injected energetic particles from the magnetotail during a substorm. Clilverd et al. (2012) described the energetic electron precipitation conditions leading to the anomaly, pointing out that a substorm injection event shortly after the shock appears to have ultimately triggered the upset on Galaxy 15.

It is well known that substorm injections and enhanced magnetospheric convection, and convection electric fields are among the key mechanisms that directly affect energetic plasma in the inner magnetosphere at geostationary orbit (Sillanpää et al., 2017). During a substorm the plasma sheet in the magnetotail is driven earthward and the encounter of an

orbiting vehicle with this plasma sheet will produce the most intense surface charging at GEO orbit (Lanzerotti et al, 1998a).

Left panel in Figure 2 shows the magnetic field x and z GSM components observations from GOES 11 and 12 from 7 to 11 UT on 5 April 2010. The vertical line is the time of the GA. Two strong dipolarizations starting at 08:47 UT and 09:03 UT (Loto´aniu et al., 2015) appear in GOES 11 data, located close to midnight. The first dipolarization is almost unnoticed by GOES 12, 60º away in longitude from GOES 11 towards dawn. The GA occurs about 45 min after the 2nd dipolarization, labeled as 'overdipolarization' in Connors et al. (2011) due to persistent Bz enhancement above usual geosynchronous values, and 60 min after the first one.

At the time of the TA the satellites available were all further than 20º in longitude from Telstar 401, but some similarities can be found between GOES 8 and 9 observations at that time and GOES 11 and 12 observations at the time of the GA. Right panel in Figure 2 shows the magnetic field x and z GSM components observations from GOES 8 and 9 from 6 to 12 UT on 11 January 1997. There is a dipolarization at GOES 9 at about 10:27 UT, while GOES 8 shows very little activity. Note also the magnetic field fluctuations observed at GOES 9 from about 7:30 UT to 12:30 UT as indicative of Ultra Low Frequency (ULF) waves. The dipolarization observed at GOES 9 coincides with the auroral brightening in the Polar image data (Figure 3). The foot of the magnetic field line through GOES 9 intercepts the Earth approximately in western Canada, just north of the bright aurora, while GOES 8 field line intercepts the Earth in eastern Canada, far to the east of the bright aurora. As in the case of GA, the analysis of observations from the GOES satellites indicates that a magnetospheric substorm took place about 45 minutes before the anomaly.

3.2 Geomagnetic Conditions from Ground-based Magnetic Field Data

Lanzerotti et al. (1998b) analyzed data from the geosynchronous (GEO) communications satellite Telstar 402R during the event on 10 January 1997, the day before the TA. Their results show that during this event enhanced plasma populations caused the charge plates to attain values more than a factor of two larger than at any other time during the month. The time variation in the surface charging on Telstar 402R during the event was found to be similar to the energy dissipation in the ionosphere as measured by the magnetic field disturbances recorded by ground magnetometers near the footpoints of the magnetic flux tube that passes through the spacecraft. This relationship between the surface charging and the ground magnetometers provides a valuable indicator of changes in the plasma population in the GEO orbit at specific locations when satellites close to the location of the anomaly are not available. In the case of Telstar 401, there are no other measurements than those provided by the three LANL and the two GOES available and all of them are too far in longitude for a suitable study.

The magnetic field near the northern footpoint of Telstar 401 is available from Baker Lake (BLC) magnetic observatory in Canada, located at 74.21º N latitude and 263.9º geographic longitude, and Gillam (GIM) magnetometer located at 66.9º N latitude and 265.4º geographic longitude. Latitudes correspond to corrected magnetic coordinates (International Geomagnetic Reference Field (IGRF) model 1995). Figure 4 shows the horizontal component intensity of the magnetic field vector recorded at BCL (top panel) and GIM (bottom panel) on 10-11 January 1997. Ionospheric currents above BLC are increased on 10 January during about hour 04 UT, between 06:30 and 09:45 UT, and between 10:30 and 14:30 UT (the first three shadowed areas in Figure 4 correspond to these intervals), and with less intensity in the

15 - 18:30 UT interval. The first and last enhancements of ionospheric currents in BLC do not appear as significant at GIM suggesting a local effect. On 11 January there is also an increase relative to the level of the previous hours of the ionospheric currents between 10:30 UT and 13:30 UT (last shadowed area in Figure 4). The corresponding signature appears in both geomagnetic observatories indicative of a non-localized effect. This plasma population is expected to produce surface charging on Telstar 401, whose failure occurred about 45 min after the beginning of enhanced ionosphere currents on 11 January. A vertical red line in Figure 4 corresponds to the time of the TA.

The nearest magnetic observatories to the northern footpoint of Galaxy 15 with data available are Deadhorse (DED) and Sitka (SIT), both in Alaska, United States (US). The geomagnetic latitude of DED is 70.14º N and that of SIT 60.20º N. Geographic longitude of the DED (SIT) observatory is 211.21º (224.67º). Magnetic latitudes are corrected by IGRF 2010 model. Plotted in Figure 5 is the H-component of the magnetic field recorded at DED (top panel) and SIT (bottom panel) on 5 April 2010. There was a sharp and brief increase in the ionospheric currents above DED between 09:00 UT and 09:50 UT. The H-component shows also large variations in SIT from 8:30 UT to 9:19 UT (shadowed area in Figure 5) with a later increase up to 10:55 UT. The magnetic field fluctuation at the peak of the event of more than 2000 nT corresponds to ionospheric currents of the order of 10^6 amperes (Lanzerotti et al., 1998b), which could be expected to trigger surface charging on Galaxy 15, whose failure occurred about 45 min after the beginning of enhanced ionosphere currents on DED.

Ground magnetic records from mid latitude observatories are also useful to identify substorms. Indeed, Field-aligned Currents (FAC) are magnetospheric currents connecting magnetosphere and ionosphere and as transferring particles injected by dipolarization of the magnetospheric field, an enhancement of ionospheric currents appears into the auroral oval, particularly the substorm current wedge (SCW) (McPherron & Chu, 2016). A clear identification of the effects at mid-latitude locations originated by FACs has been pointed out in Cid et al. (2015) and Saiz et al. (2016) as the day-night asymmetry of the magnetic disturbance of short time (negative bay at the dayside but positive in the nightside). Figure 6 shows the H-component of the magnetic field from San Pablo-Toledo (SPT), Spain (top panels) and Fresno (FRN), US (bottom panels) on the day of the anomaly (left: Telstar, right: Galaxy). Both magnetic observatories are at about 40º N geomagnetic latitude. At the observatory sites, geomagnetic local time is LT_{SPT} = UT + 0h and LT_{FRN} = UT - 8h, respectively. Therefore, at the time of both anomalies, SPT was close to prenoon and FRN was close to postmidnight. Shadowed areas in Figure 6 correspond to the time interval where magnetic disturbances due to ionospheric currents appear both at BLC and GIM (left panel), and DED and SIT (right panel), (see above and Figures 4 and 5).

As can be appreciated in Figure 6, during these substorm intervals time (as previously identified by the magnetic records at the footpoint of the spacecraft) negative bays appear in SPT records and positive spikes appear in FRN. This day-night asymmetry observed at mid latitudes, indicative of substorm, reinforces above results based on the records at the footpoints of the magnetic flux tube that passes through the spacecraft.

4 IP Signatures Triggering Substorms During the Events

This section analyzes the solar wind and interplanetary magnetic field (IMF) conditions, to identify their roles in substorm triggering during the events on 11 January 1997 and 5 April 2010 related to the TA and the GA. The data source for the January 1997 event is

the Wind spacecraft. At that time Wind is located upstream of the Earth at the L1 point. Magnetic field data are from the Wind/MFI instrument (Lepping et al., 1995) and the solar wind plasma data from Wind/SWE (Ogilvie et al., 1995). For the April 2010 event, magnetic field data are obtained from ACE/MAG (Smith et al., 1998) and plasma from ACE/SWEPAM (McComas et al., 1998).

Figure 7 shows the solar wind and IMF conditions (B, By, Bz, V, Pdyn) during 5 April 2010. Superimposed on a solar wind background flow of 500-600 km/s speed appears the interplanetary counterpart of the coronal mass ejection (CME) launched on 3 April, with a leading edge travelling at 725 km/s. With the arrival of this transient at 08 UT, IMF Bz turned strongly negative (< -10 nT) with a By component of somewhat greater than 5 nT. Simultaneously solar wind dynamic pressure enhanced from 2 to 10 nPa. Over the next hour, Bz remained southward and almost steady in average. Nevertheless, several small abrupt decreases on the southern Bz can be noticed before turning suddenly northward at 09 UT. Then Bz remained northward for about 15 min. During this interval there was an enhancement of solar wind dynamic pressure and a reduction of the IMF By from 08:30 UT.

The response of the magnetosphere to those interplanetary conditions described above was as follows: the cross-tail current sheet intensified and the magnetic field at geostationary orbit became stressed and tail-like; this process of magnetic field stretching into the magnetosphere ceased abruptly and the configuration of field line changed from a tail-like to a more dipole-like orientation. Then the two dipolarizations observed by GOES take place and start the expansion phase of substorm. Both dipolarizations were related to the small abrupt decreases of the southern Bz described above. The observed increase in magnetospheric Bz (and decrease in Bx) at 9:20 UT, soon after the second and more intense dipolarization, corresponded to the northward turning of IMF Bz (see left panel in Figure 2).

In short, the interplanetary scenario described above provided the essential conditions to trigger a substorm observed in the magnetosphere as a magnetic field dipolarization, and injection of energy into the ionosphere (observed at DED and SIT before the GA). Indeed, the shadowed area in Figure 7 corresponds to the interval of increased ionospheric currents shadowed in Figure 5, about 30 minutes ahead considering ACE data propagation.

Solar wind parameters and IMF during 9-11 January 1997 are shown in Figure 8. On 10 January at 00:40 UT an IP shock disturbed the quiet solar wind reaching the Wind spacecraft. The driver of this shock was a magnetic cloud travelling at 450 km/s, where the IMF gradually rotated from strongly southward (< -10 nT) to northward while magnetic field strength remained nearly constant. Ahead of the flux rope, a fluctuating Bz with a strength of 5 nT appeared in the sheath. Behind the magnetic cloud, an interaction region preceded a fast stream reaching Wind during the second half of 11 January. The large proton density value (> 150 cm^{-3}) reached at the rear of the magnetic cloud, one of the largest ever observed, provides a signature of the interaction between the magnetic cloud and the fast stream (Cid et al., 2016).

The four shadowed areas in Figure 8 correspond to the intervals with increased ionospheric currents above BLC and GIM shadowed in Figure 4 (90 min ahead by considering Wind data propagation). During all those intervals Bz was southward, enhancing the cross-tail current sheet. The southward turnings of IMF happened at the beginning of three out the four shadowed areas (on 10 January at ≈ 02 UT and ≈ 05 UT, and on 11 January at 09:30 UT after a long period of about 12 hours under northward Bz), being By positive during these whole three intervals. Regarding the other shadowed area, the southward IMF component started to

decrease at the beginning of the interval, on 10 January at ≈09 UT. However, By was negative in this case. During the four shadowed areas the solar wind pressure was not larger than 5 nPa.

5 The Operational History of the Spacecraft and the Anomalies

The relevance of the conditions described above requires a comparison of the conditions at the date of the anomaly to conditions throughout the operational history of the spacecraft. Figures 9 and 10 show historical solar wind conditions during the whole mission of Galaxy 15 and Telstar 401, respectively and the historical AL index (as indicative of global substorms). Relevant parameters involved in the process of triggering a substorm appear from top to bottom: the interplanetary electric field and the solar wind dynamic pressure Pdyn (as indicative of convection in the magnetosphere and compression, in order to identify intensifications of the cross-tail current sheet), the variation of the IMF Bz (to identify northward turnings), and the variation of the IMF |By| (to identify decreases in the amplitude of the IMF By component) (Hsu & McPherron, 2003; Peng et al., 2013). Data for Figure 9 and 10 are 5-minute resolution from the OMNI web database (https://omniweb.gsfc.nasa.gov/), and therefore, shifted to the Earth's bow shock nose. The variation of the IMF Bz and By corresponds to the change in those parameters from one data (in 5-minute resolution) to the previous one. Dashed horizontal lines indicate the maximum value of the parameter in the corresponding plot just prior to the respective satellite anomalies. Note that those maximum values might not be reached simultaneously by the different parameters, but all of them are outlined against background few minutes (or hours) before the anomaly.

A study of the operational history of Galaxy 15 was previously performed by Loto´aniu et al., (2015), but that study was not focused on the IP parameters able to trigger substorms, but in those parameters related to large planetary geomagnetic disturbances like the Kp index.

Before the anomaly of Galaxy 15, the most outstanding record of those in Figure 9, when compared to the whole mission, is the dawn to dusk convection electric field, Ey, which reached 9.40 mV/m on 5 April at 08:30 UT. The AL index reached less than -2000 nT one hour later of the arrival of that large Ey to the terrestrial environment, indicating that a global substorm was developed. At that time the spacecraft was at local midnight, i.e., immersed in the cross-tail current sheet. The GA occurred about 1.5 hours later. Only one previous event was recorded with larger Ey (14.4 mV/m): during the 14-15 December 2006 geomagnetic storm. Although the other parameters plotted were also large before the failure, they cannot be considered extraordinary. However, the fact that all of them were large at the same time should be also considered.

Regarding the Telstar 401 anomaly, Δ|By| was the outstanding parameter, although, as in the Galaxy failure, all the other parameters in Figure 10 were also large at some previous moments (in a time interval of a few hours) to the anomaly. The amplitude of By changed 13.91 nT from 06:00 UT to 06:05 UT on 11 January, but this large change corresponds to an increase in the amplitude of By. Two reductions of IMF |By| of 11.7 nT occurred at 05:15 and 06:00 UT the same day. Telstar 401 was at that time also close to local midnight, i.e., immersed in the cross-tail current sheet. The TA ocurred about 5 hours later. As in the case of Galaxy 15, on January 11 from 10:30 UT the AL index also showed substorm activity, although less intense. It should be noted that a gap in the solar wind plasma data in OMNIWeb database misses a large pressure pulse before the anomaly. This enhanced

pressure will be obtained because of the large enhancement in the proton density measured by Wind spacecraft, and shown in Figure 8, but it is missed in Figure 10. It would mean that a bigger threshold for Pdyn would appear in the second panel (about 38 nPa).

Only one event, on 21 February 1994, Δ|By| and Pdyn reached values larger than before the TA (about -25 nT and 46 nPa, respectively). Considering just the reductions of IMF By (Δ|By|< 0), two other events appear: on 02 May 1994 and on 24 December 1995.

6 Discussion and Conclusions

About the two events analyzed regarding satellite anomalies related to ESD, several similarities and differences have been discovered, both in the geomagnetic conditions and in the interplanetary signatures.

Regarding geomagnetic conditions, spacecraft-charging hazards have been characterized by Kp (e.g. Thomsen et al., 2013; Denton et al., 2016), but both events largely differ when considering Kp. The extreme values during the GA (up to Kp = 8^- in a scale ranging from 0 to 9) were not comparable to the minor activity during the TA, when Kp index reached just 4. Our results agree with those from Bodeau (2015) when stating that 'Kp in this case was absolutely misleading'. Indeed, Kp passed 8 in eight occasions during the lifetime of Telstar 401. The main problem of Kp as a proxy in this case is its low temporal resolution (3-hours) and the planetary character of the index, which misses the short-time and local signature of some magnetic disturbance as FACs.

On the contrary, local geomagnetic records, both from GOES satellites and from ground records, reveal that both anomalies took place during the expansion phase of a triggered substorm, ≈ 45 minutes after a dipolarization of the geomagnetic field. The magnetic effects of FACs as seen by the enhancements of ionospheric currents and the corresponding ground magnetic disturbances were also observed at mid/low latitude stations during both events. Thus, this study clarifies the origin of the positive disturbance recorded by a low/mid latitude geomagnetic observatory located at night side, which was previously explained as a 'magnetospheric reconfiguration' by Denig et al. (2010). This distinct signature (a day-night asymmetry of the magnetic field observed at mid-latitude stations) is revealed as an unmistakable indicator of substorms occurring of significant intensity instead of the classic indices AL and AE, particularly interesting when observations from space are limited as was the case of TA. Even more, the AL index, commonly used as a substorm proxy, not was relevant in this analysis, for example, in the selection of thresholds during the whole mission of the spacecraft, as some substorms can be missed by this geomagnetic index.

Even if both events were similar in having dipolarizations less than an hour before each anomaly, the dipolarizations were not comparable. In the case of Galaxy 15 two strong dipolarizations (one of them, the closest in time to the anomaly, labeled as 'overdipolarization' in Connors et al. (2011)) occurred whereas the dipolarization before the TA was not as intense in the GOES data records.

Also, the magnetic disturbances recorded at the footpoint of Galaxy 15 were larger than those 45 min ahead the TA, but in the case of TA, previous substorm activity is clearly identified on 10 January 1997 (the day before the anomaly) when Telstar 401 was again at the night sector, crossing the magnetotail. The magnitude of this substorm activity, according to the H-component recorded at the nearest magnetic observatories to the northern footpoint of Telstar 401, was comparable to that happened on 05 April 2010 before the Galaxy anomaly.

Considering the slow recovery to quiet time of the voltage recorded on the charge plate of another Telstar spacecraft (see central panel of Figure 2 of Lanzerotti et al. (1998a) for the registered potential of Telstar 402R during the January 10 storm), the dipolarization at 10:30 UT on 11 January 1997 in Telstar 401, located only 8º West from Telstar 402R, can be considered as 'the last straw that broke the camel's back'.

The analysis of Wind and ACE spacecraft data to identify the interplanetary triggers of the substorms before these spacecraft anomalies also reveals some similarities. In both cases, the interplanetary counterpart of a coronal mass ejection interacted with a high-speed stream. As a result, the substorm triggers were favored. The interaction resulted in a dynamic pressure enhanced, and an interplanetary magnetic field enhanced and fluctuating as well.

An assessment of the parameters related to substorms through the operational history of the spacecraft has shown that some of them were extreme before the anomalies. Specifically, the interplanetary electric field, Ey, and the geomagnetic index AL were large in both cases, and the variation of the amplitude of By was extraordinary in the case of Telstar 401. Regarding other outstanding events during the operational history of the Galaxy 15, Ey and AL reached the high levels observed on 5 April 2010 only during the storm on 14 - 15 December 2006. The transient that triggered this storm was likely a magnetic cloud preceded by a high speed stream, developing a sheath with a largely fluctuating IMF, as can be deduced from the large values of the parameters shown in Figure 9. However, when checking the location of the spacecraft at the time of the most disturbed conditions in the magnetosphere, while the main phase of the storm is developed, we find that Galaxy 15 was on the dayside. Moreover, there was no significant dipolarization observed by GOES when Galaxy 15 was near midnight during this storm.

Regarding other outstanding events during the operational history of the Telstar 401, only one event, at 16:35 UT on 21 February 1994, $\Delta|By| > 0$ was larger prior to the TA. The large data gaps in interplanetary data during this event do not allow us to analyze the relevance of this event in the operational history of Telstar 401.

Considering just the reductions of IMF |By|, two other outstanding events ($\Delta|By| < -10$ nT) appear during the operational history of Telstar: 02 May 1994 and 24 December 1995. On 02 May 1994, the reduction on the amplitude of By took place at 16:15 UT after a northward turning of IMF, but Telstar was at 10 MLT, again far from the magnetotail currents. The event on 24 December 1995 deserves more attention. A moderate geomagnetic storm occurred on that day, with the Kp index reaching 5. Auroral activity was also moderate from 07 UT to 11 UT (AL reached a peak value in that interval of -800 nT at 10 UT). During this interval Telstar locations were between 0.5 and 4.5 MLT, i.e., the same as the anomaly of January 1997. Also, both events happened in winter (with a separation of 18 days) and during the minimum of the Solar Cycle 22. This scenario might suggest that similar geomagnetic conditions resulted in different consequences. However, deeper analysis will reveal the differences. Later, from 11:30 UT, the substorm activity on 24 December was enhanced, reaching a peak value of -1200 nT at 14:40 UT. At that time, Telstar was on the dayside.

On 24 December 1995 $\Delta|By|$ reached -12.33 nT at 08:45 UT, and -12.38 nT at 09:05 UT, i.e., when Telstar was located at 2:15 MLT. Ey passed the threshold of 7 mV/m three times: at 07 UT, 08:30 UT and 10 UT. Therefore, when convection was reinforced, the spacecraft was in the morning sector. GOES 8 and 9 observed dipolarizations in magnetic field at 07 UT, 08:30 UT and 10 UT. The times of these dipolarizations were similar to these of the event on 11 January 1997, therefore, the satellite was in the same local sector when

they took place. From 06 UT to 09 UT on 24 December, dynamic pressure also reached high values (about 24 nPa). Therefore, we have to conclude that on 24 December 1995 there were enough interplanetary conditions to trigger a substorm which can explain the extreme conditions forcing the magnetosphere where the spacecraft was immersed one year after its launch. However, the spacecraft survived those adverse conditions.

Despite the similarities described above, there are also some differences that provide the key to explain why the TA happened during the January 1997 event. First, the interplanetary transient of the 1995 event was just an interaction region (IR) and the solar wind conditions preceding the IR corresponded to those of quiet time: average IMF strength, Bz IMF and Pdyn are 6 nT, 0 nT and 5 nPa, respectively. In contrast, in the 1997 event a magnetic cloud was preceding the fast stream, largely disturbing the solar wind conditions at the IR ahead of the fast stream.

Other differences concern the inner conditions of the magnetosphere. On one hand, there were large differences in the proton and electron flux values measured at GEO orbit by GOES 8 and 9 (not shown) during those "critical hours". The electron flux values were much larger in 1997 (by a factor of about 15). On the other hand, in the 1995 event the dipolarizations were evident in both GOES 8 and GOES 9 data records during the time interval of interest. However, dipolarizations were only detected at GOES 9 during the 1997 event. This asymmetry in the magnetic field observed by the two GOES is indicative of a local magnetic disturbance, with the subsequent local particle injection. In 1997, Telstar was located between GOES 8 and GOES 9, supporting that it was located in an unsuitable location, due to the asymmetric configuration of the magnetosphere at that time.

There are several previous studies on the influence of one of the components of the IMF in the entrance of energy from the solar wind to the magnetosphere-ionophere system and on the asymmetries associated with the relevant role played by any IMF component by minimizing the role of the others (Ostgaard et al., 2003, 2004; Liou et al, 2006; Belenkaya et al., 2007; Cheng et al., 2007, 2018; Tenfjord et al., 2015; Wing et al. 2010; Chakrabarty et al., 2017). However, the IMF influence on the FACs in the magnetotail should be a combined contribution of all IMF components and not only from a single one (Cheng et al., 2013).

In the interval of interest in 1997, i.e., from when GOES 9 observes the dipolarization until the time of the anomaly, 10:30 UT - 11:15 UT, Telstar 401 was located at 4 - 4.75 MLT. From the sign and the magnitude of the IMF components in this time interval, the asymmetry angle γ, defined as $\tan(\gamma) = -By/Bx$ (Belenkaya et al., 2007), was positive indicating a significant shift ($\approx$ 4-5 hours) of the magnetospheric field lines, which displaced the FAC current circuit from midnight to dawn. Additionally, the cone angle θ, defined as $\cos(\theta) = |Bx|/B$ (Cheng et al., 2013), was larger than 80º. This cone angle is well related to the FAC occurrence rate, especially for Northern Bz IMF conditions, keeping this rate high when the angle is high, as in this case. Also the clock angle ϕ, defined as $\tan(\phi) = By/Bz$ is -55º, which was very close to $|\phi| \approx 60º$ pointed out by Cheng et al. (2013) as lower limit for large FAC densities. On the other hand, the magnitude of IMF By and Bz were comparable and both larger than IMF Bx, therefore they were the IMF components playing a relevant role in the magnetic configuration of the magnetosphere at that time. All the above allows us to conclude that Telstar was in an unsuitable location at the time of the anomaly.

Summarizing all the above, the two events related to ESD anomalies studied in this paper, GA and TA, happened as a consequence of a dipolarization of the magnetosphere

triggering a substorm when the spacecraft were located in the sector 0-6 MLT. Nevertheless both events present relevant differences that need to be considered to raise awareness of potential space weather hazards for spacecraft in GEO orbit. Below we highlight the most important differences:

1. The day before the GA there were no particularly adverse interplanetary conditions for a nominally benign environment, being the IMF strength about 5 nT, which is a typical value for quiet time. The magnetic activity involved in the GA happened during the first two hours after the arrival of an interplanetary transient (a compressed magnetic cloud) to a quiet magnetosphere. The trigger of the second, and more intense, dipolarization was a northward turning of a large southern IMF Bz (-10 nT). Meanwhile the magnitude of IMF Bz and By components were similar, but with opposite sign ($Bz < 0$ and $By > 0$). Under the first hour with intense southward Bz, the magnetospheric convection was reinforced, $Ey > 0$, with the subsequent significant entrance of the energy from solar wind to the magnetosphere and partially released as a substorm.

   In contrast, the day before the TA there was a moderate storm which resulted in a preconditioning of the magnetosphere, which can be noticed, for example, in the steady but enhanced flux of relativistic electrons and protons, or in the reinforced electron flux in the energy range 50 - 75 keV on 11 January until 12 UT (Reeves et al., 1998), that is when the substorm recovery phase began. The scenario for this event close to the time of the TA can be described as follows: the magnetosphere was strongly stressed for a long time and then, when Bz turned southward, although not being so large in magnitude, keeping southward for about one hour, energized the magnetosphere and initiated substorm processes. The large asymmetry of the magnetosphere results in a deviation of the particle flux injection towards dawn sector MLTs, where Telstar was located.

2. The activity which resulted in the TA is described by the interplanetary conditions resulting from the interaction between a high speed stream and the preceding magnetic cloud, which caused the geomagnetic storm on 10 January 1997. This interaction resulted in a reinforced profile for the magnetic field strength at the trailing part of the magnetic cloud (Farrugia et al., 1998) which caused an extraordinarily large pressure pulse. Afterwards, an intense but northward IMF persisted for about 12 hours which limited the energy input to the magnetosphere. Nevertheless, there is a large compression of the magnetosphere as both dynamic and magnetic solar wind pressure were relevant. This large solar wind pressure affects the spatial configuration of the inner magnetosphere and other IMF components aside from Bz start to play a major role in the magnetospheric dynamics as explained above.

3. The relevant solar wind parameter before the anomaly of the Galaxy 15, in the context of its operational history, was the dawn-dusk electric field, however in the case of Telstar 401 the most important parameters were |By| and dynamic pressure.

4. The substorm injections may produce ULF waves in the dipolar magnetosphere (Borovsky & Yakymenko, 2017). These ULF waves were observed in the event of January 1997 but not in the event of 2010.

In summary, the Telstar and Galaxy anomalies occurred under particular geomagnetic conditions, requiring a very specific combination of events. In both cases the

spacecraft crossed the magnetotail during a large substorm activity, and then another dipolarization took place at the spacecraft location, indicating that, as previously said by Allen (2010) for the Galaxy 15, Telstar was also 'another satellite in the wrong place at a critical time'.

Future work should be dedicated to search for better proxies of geomagnetic conditions than Kp or AL as identifiers of potential charging hazards. Considering the results of this paper, indices related to day-night asymmetry of magnetic disturbance at mid latitudes will be a good starting point, but a wider list of ESD anomalies will be needed for this purpose.

Acknowledgments

This work has been funded by the Spanish Ministerio de Economía y Competitividad (MINECO) under project AYA2016-80881-P (including AEI/FEDER funds, EU). The authors acknowledge all data sources used for this study: from GFZ, GOES, Polar, Wind MFI and SWE, ACE MAG and SWEPAM, and OMNI database. We acknowledge SuperMAG (http://supermag.jhuapl.edu/mag/) for providing access to the one-minute resolution measurements of the ground magnetic field at BLC, GIM, DED and SIT, and INTERMAGNET (http://www.intermagnet.org/) for providing access to the one-minute resolution measurements of the ground magnetic field at SPT and FRN, and acknowledge to the staff at those ground bases magnetometers for recording the data. We thank D. Pitchford and W. Denig for their assistance in evaluating this paper.

References

Allen, J. (2010), The Galaxy 15 anomaly: Another satellite in the wrong place at a critical time, *Space Weather*, 8 (6), doi:10.1029/2010SW000588.

Anderson, P. C. (2012), Characteristics of spacecraft charging in low Earth orbit, *Journal of Geophysical Research: Space Physics*, 117 (A7), doi:10.1029/2011JA016875.

Belenkaya, E. S., Alexeev, I. I., & Clauer, C. R. Jr. (2007), Magnetic field of the transition current system: dawn-dusk asymmetry, *Annales Geophysicae*, 25 (8), 1899–1911, doi:10.5194/angeo-25-1899-2007.

Bodeau, M. (2015), Review of better space weather proxies for spacecraft surface charging, *IEEE Transactions on Plasma Science*, 43 (9), 3075–3085, doi:10.1109/TPS.2015.2441038.

Borovsky, J. E., & Yakymenko, K. (2017), Substorm occurrence rates, substorm recurrence times, and solar wind structure, *Journal of Geophysical Research: Space Physics*, 122 (3), 2973–2998, doi:10.1002/2016JA023625.

Chakrabarty, D., Hui, D., Rout, D., Sekar, R., Bhattacharyya, A., Reeves, G. D., & Ruohoniemi, J. M. (2017), Role of IMF By in the prompt electric field disturbances over equatorial ionosphere during a space weather event, *Journal of Geophysical Research: Space Physics*, 122 (2), 2574–2588, doi:10.1002/2016JA022781.

Cheng, Z.-W., Shi, J. K., Zhang, T.-L., & Liu, Z.-X. (2007), Probability of field-aligned currents observed by the satellite Cluster in the magnetotail, *Chinese Physics Letters*, 24 (4), 1125.

Cheng, Z. W., Shi, J. K., Dunlop, M., & Liu, Z. X. (2013), Influences of the interplanetary magnetic field clock angle and cone angle on the field-aligned currents in the magnetotail, *Geophysical Research Letters*, 40 (20), 5355–5359, doi:10.1002/2013GL056737.

Cheng, Z. W., Shi, J. K., Zhang, J. C., Torkar, K., Kistler, L. M., Dunlop, M., et al. (2018), Influence of the IMF cone angle on invariant latitudes of polar region footprints of FACs in the magnetotail: Cluster observation, *Journal of Geophysical Research: Space Physics*, 123 (4), 2588–2597, doi:10.1002/2017JA024941.

Choi, H.-S., Lee, J., Cho, K.-S., Kwak, Y.-S., Cho, I.-H., Park, Y.-D. et al. (2011), Analysis of GEO spacecraft anomalies: Space weather relationships, *Space Weather*, 9 (6), doi:10.1029/2010SW000597.

Cid, C., Saiz, E., Guerrero, A., Palacios, J, & Cerrato, Y. (2015), A Carrington-like geomagnetic storm observed in the 21st century, *Journal of Space Weather and Space Climate*, 5, A16, doi:10.1051/swsc/2015017.

Cid, C., Palacios, J., Saiz E., & Guerrero, A. (2016), *Astrophysical Journal*, 828, doi:10.3847/0004-637X/828/1/11

Clilverd, M. A., Rodger, C. J., Danskin, D., Usanova, M. E., Raita, T., Ulich, T., Spanswick, M. L. (2012), Energetic particle injection, acceleration, and loss during the geomagnetic disturbances which upset Galaxy 15, *Journal of Geophysical Research: Space Physics*, 117, doi:10.1029/2012JA018175.

Connors, M., Russell, C. T., &. Angelopoulos, V. (2011), Magnetic flux transfer in the 5 April 2010 Galaxy 15 substorm: an unprecedented observation, *Annales Geophysicae*, 29 (3), 619–622, doi:10.5194/angeo-29-619-2011.

Denig, W., Green, J., Wilkinson, D., Rodriguez, J., Singer, H., Loto'Aniu, P., et al. (2010), Space weather conditions at the time of the Galaxy 15 spacecraft anomaly, in *AGU Fall Meeting Abstracts*.

Denton, M. H., Henderson, M. G., Jordanova, V. K., Thomsen, M. F., Borovsky, J. E., Woodroffe, J., et al. (2016), An improved empirical model of electron and ion fluxes at geosynchronous orbit based on upstream solar wind conditions, *Space Weather*, 14 (7), 511–523, doi:10.1002/2016SW001409.

Farrugia, C. J., Scudder, J. D., Freeman, M., Janoo, L., Lu, G., Quinn, J. M., et al. (1998), Geoeffectiveness of three WIND magnetic clouds: A comparative study, *Journal of Geophysical Research: Space Physics*, 103 (A8), 17,261–17,278, doi:10.1029/98JA00886.

Farthing, W., Brown, J., & Bryant, W. (1982), Differential spacecraft charging on the geostationary operational environmental satellites, *NASA STI/Recon Technical Report Nº 82*.

Ferguson, D., Denig, W., & Rodriguez, J. (2011), Plasma conditions during the Galaxy 15 anomaly and the possibility of ESD from subsurface charging, in *49th AIAA Aerospace Sciences Meeting including the New Horizons Forum and Aerospace Exposition*, p. 1061.

Garrett, H. B., & Whittlesey, A. C. (2000), Spacecraft charging, an update, *IEEE Transactions on Plasma Science*, 28 (6), 2017–2028, doi:10.1109/27.902229.

Green, J. C., Likar, J., & Shprits, Y. (2017), Impact of space weather on the satellite industry, *Space Weather*, 15 (6), 804–818, doi:10.1002/2017SW001646.

Hsu, T., & McPherron, R. L. (2003), Occurrence frequencies of IMF triggered and nontriggered substorms, *Journal of Geophysical Research: Space Physics*, 108 (A7), doi:10.1029/2002JA009442.

Iucci, N., Levitin, A. E., Belov, A. V., Eroshenko, E. A., Ptitsyna, N. G., Villoresi, G., et al. (2005), Space weather conditions and spacecraft anomalies in different orbits, *Space Weather*, 3 (1), 1–16, doi:10.1029/2003SW000056.

Koons, H. C., Mazur, J. E., Selesnick, R. S., Blake, J. B., Fennell, J. F., Roeder, J. L., & Anderson, P. C. (1998), The Impact of the Space Environment on Space Systems, in *6th Spacecraft Charging Technology*, pp. 7–11.

Lanzerotti, L., Breglia, C., Maurer, D., Johnson, G., &. Maclennan, C. (1998a), Studies of spacecraft charging on a geosynchronous telecommunications satellite, *Advances in Space Research*, 22 (1), 79–82, doi:https://doi.org/10.1016/S0273-1177(97)01104-6, solar-Terrestrial Relations: Predicting the Effects on the Near-Earth Environment.

Lanzerotti, L. J., LaFleur, K, Maclennan, C. G., & Maurer, D. W. (1998b), Geosynchronous spacecraft charging in January 1997, *Geophysical Research Letters*, 651 25 (15), 2967–2970, doi:10.1029/98GL00987.

Lepping, R. P., Acuña, M. H., Burlaga, L. F., Farrell, W. M., Slavin, J. A., Schatten, K. H., et al. (1995), The WIND magnetic field investigation, *Space Science Reviews*, 71 (1), 207–229, doi:10.1007/BF00751330.

Liou, K., Meng, C., & Wu, C. (2006), On the interplanetary magnetic field by control of substorm bulge expansion, *Journal of Geophysical Research: Space Physics*, 111 (A9), doi:10.1029/2005JA011556.

Loto'aniu, T. M., Singer, H. J., Rodriguez, J. V., Green, J., Denig, W., Biesecker, D., & Angelopoulos, V. (2015), Space weather conditions during the Galaxy 15 spacecraft anomaly, *Space Weather*, 13 (8), 484–502, doi:10.1002/2015SW001239.

McPherron, R. L., & Chu, X. (2016), *Geoscience Letters*, 3:12, doi: 10.1186/s40562-016-0044-5.

McComas, D., Bame, S., Barker, P., Feldman, W., Phillips, J., Riley, P., & Griffee, J. (1998), Solar wind electron proton alpha monitor (SWEPAM) for the advanced composition explorer, *Space Science Reviews*, 86 (1), 563–612, doi:10.1023/A:1005040232597.

O'Brien, T. P. (2009), SEAES-GEO: A spacecraft environmental anomalies expert system for geosynchronous orbit, *Space Weather*, 7 (9), 1–14, doi:10.1029/2009SW000473.

Ogilvie, K. W., Chornay, D. J., Fritzenreiter, R. J., Hunsaker, F., Keller, J., Lobell, J., et al. (1995), Swe, a comprehensive plasma instrument for the wind spacecraft, *Space Science Reviews*, 71 (1), 55–77, doi:10.1007/BF00751326.

Ostgaard, N., Mende, S. B., Frey, H. U., Frank, L. A., & Sigwarth, J. B. (2003), Observations of nonconjugate theta aurora, *Geophysical Research Letters*, 30 (21), doi:10.1029/2003GL017914.

Ostgaard, N., Mende, S. B., Frey. H. U., Immel, T. J., Frank, L. A., Sigwarth, J. B., & Stubbs, T. J. (2004), Interplanetary magnetic field control of the location of substorm onset and auroral features in the conjugate hemispheres, *Journal of Geophysical Research: Space Physics*, 109 (A7), doi:10.1029/2003JA010370.

Ozkul, A., Lopatin, A., Shipp, A., Pitchford, D., Mazur, J. E., Roeder, J. L., et al. (2001), Initial Correlation Results of Charge Sensor Data from Six INTELSAT VIII Class Satellites with Other Space and Ground Based Measurements, in *Spacecraft Charging Technology*, *ESA Special Publication*, vol. 476, edited by R. A. Harris, p. 293.

Peng, Z., Wang, C., Yang, Y. F., Li, H., Hu, Y. Q., & Du, J. (2013), *Journal of Geophysical Research: Space Physics*, 118, 364–374, doi:10.1029/2012JA018065.Reeves, G. D., Friedel, R. H. W., Belian, R. D., Meier, M. M., Henderson, M. G., Onsager, T., et al. (1998), The relativistic electron response at geosynchronous orbit during the January 1997 magnetic

storm, *Journal of Geophysical Research: Space Physics*, 103 (A8), 17,559–17,570, doi:10.1029/97JA03236.

Saiz, E., Guerrero, A., Cid, C., Palacios, J., & Cerrato, Y. (2016), Searching for Carrington-like events and their signatures and triggers, *Journal of Space Weather and Space Climate*, 6, A6, doi:10.1051/swsc/2016001.

Sillanpää, I., Ganushkina, N. Y., Dubyagin, S., & Rodriguez, J. V. (2017), Electron fluxes at geostationary orbit from GOES MAGED data, *Space Weather*, 15 (12), 1602–1614, doi:10.1002/2017SW001698.

Smith, C., L'Heureux, J., Ness, N., Acuña, M., Burlaga, L., &. Scheifele, J. (1998), The ACE Magnetic Fields Experiment, *Space Science Reviews*, 86 (1), 613–632, doi:10.1023/A:1005092216668.

Tenfjord, P., Ostgaard, N., Snekvik, K., Laundal, K. M., Reistad, J. P., Haaland, S., & Milan, S. E. (2015), How the IMF By induces a By component in the closed magnetosphere and how it leads to asymmetric currents and convection patterns in the two hemispheres, *Journal of Geophysical Research: Space Physics*, 120 (11), 9368–9384, doi:10.1002/2015JA021579.

Thomsen, M. F., Henderson, M. G., & Jordanova, V. K. (2013), Statistical properties of the surface-charging environment at geosynchronous orbit, *Space Weather*, 11 (5), 237–244, doi:10.1002/swe.20049.

Vampola, A. L. (1994), Analysis of environmentally induced spacecraft anomalies, *Journal of Spacecraft and Rockets*, 31, 154–159, doi:10.2514/3.26416.

Wilkinson, D. C. (1994), National Oceanic and Atmospheric Administration's spacecraft anomaly data base and examples of solar activity affecting spacecraft, *Journal of Spacecraft and Rockets*, 31, 160–165, doi:10.2514/3.26417.

Wing, S., Ohtani, S., Newell, P. T., Higuchi, T., Ueno, G., & Weygand, J. M. (2010), Dayside field-aligned current source regions, *Journal of Geophysical Research: Space Physics*, 115 (A12), doi:10.1029/2010JA015837.

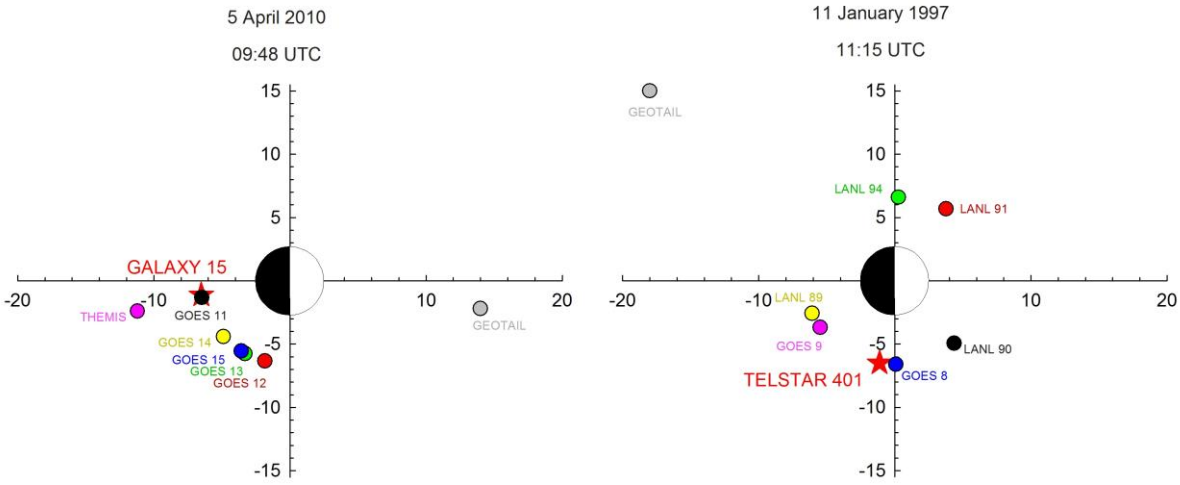

Figure 1. Relative location of spacecraft in GSM XY plane (in R_E) for the time of (a) Galaxy 15 anomaly and (b) Telstar 401 anomaly.

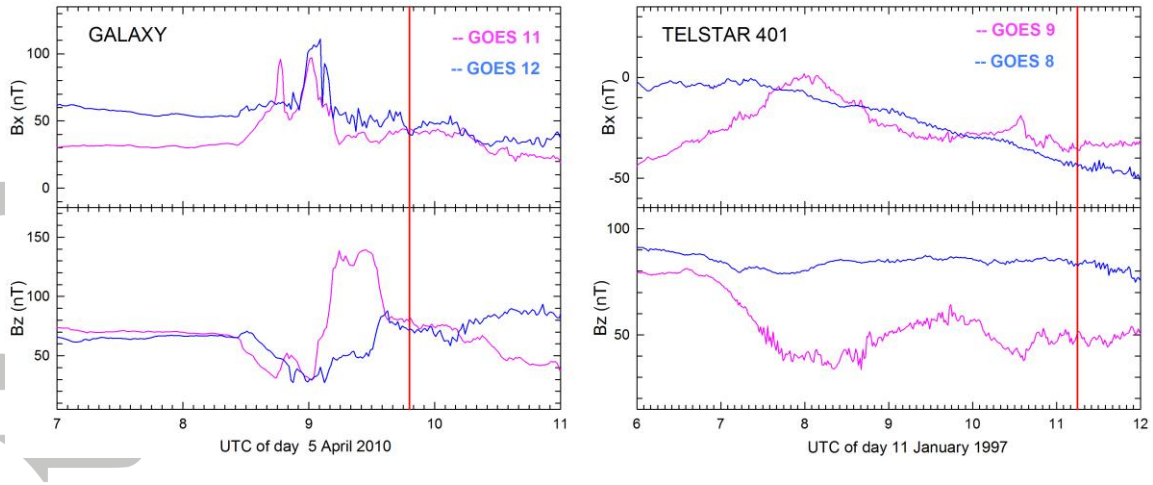

Figure 2. The GOES magnetic field observations: Bx and Bz GSM components for 5 April 2010, over 07-11 UT (left) and Bx and Bz GSM components for 11 January 1997, over 08-12 UT (right). Red vertical line marks the time of each anomaly.

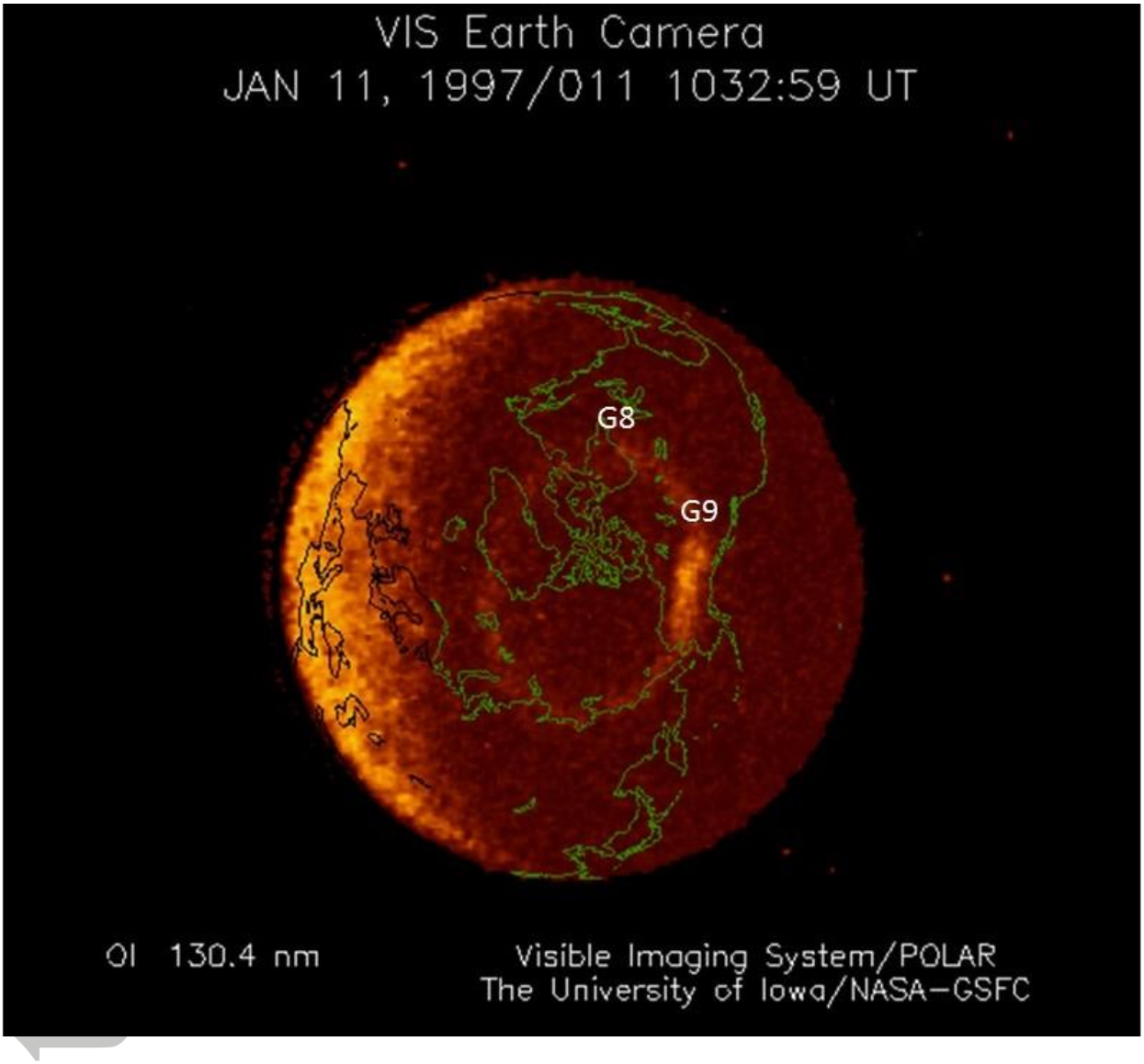

Figure 3. Image acquired with the Visible Imaging System (VIS) Earth Camera on board the Polar satellite on 11 January 1997 at 10:32:59 UT from the Polar VIS Image Archive at the University of Iowa. G8 and G9 (over plot in white) correspond to the foot points of GOES 8 and GOES 9, respectively.

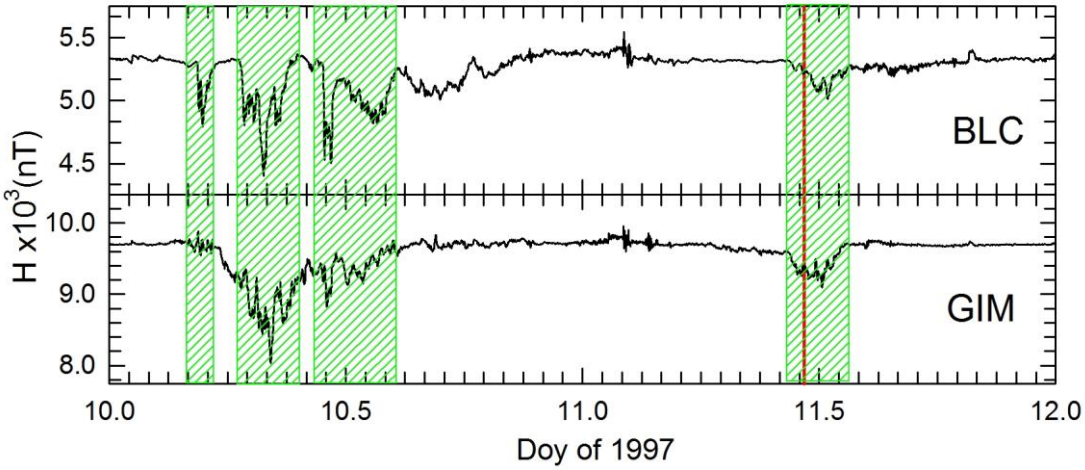

Figure 4. H-component of the magnetic field recorded at BLC and GIM high-latitude stations on 10-11 January 1997. Shadowed areas correspond to the intervals with ionospheric current enhancements.

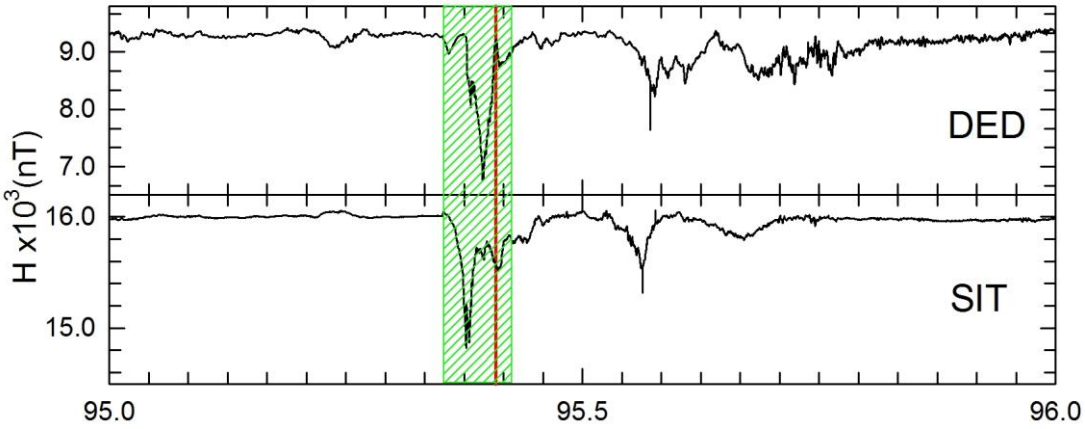

Figure 5. H-component of the magnetic field recorded at DED and SIT high-latitude stations on 5 April 2010 (Doy 95). Shadowed area corresponds to the interval with ionospheric current enhancement.

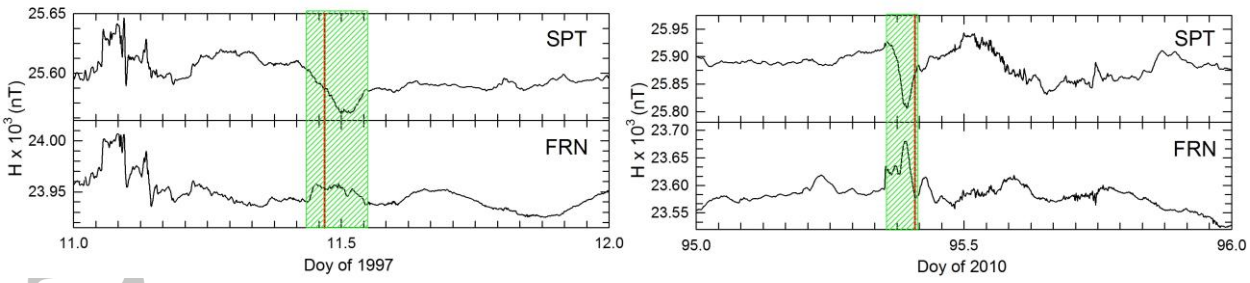

Figure 6. Horizontal component of the magnetic field recorded at SPT and FRN mid-latitude observatories on 11 January 1997 (left) and 5 April 2010 (right). Shadowed areas correspond to those in Figure 4 and Figure 5.

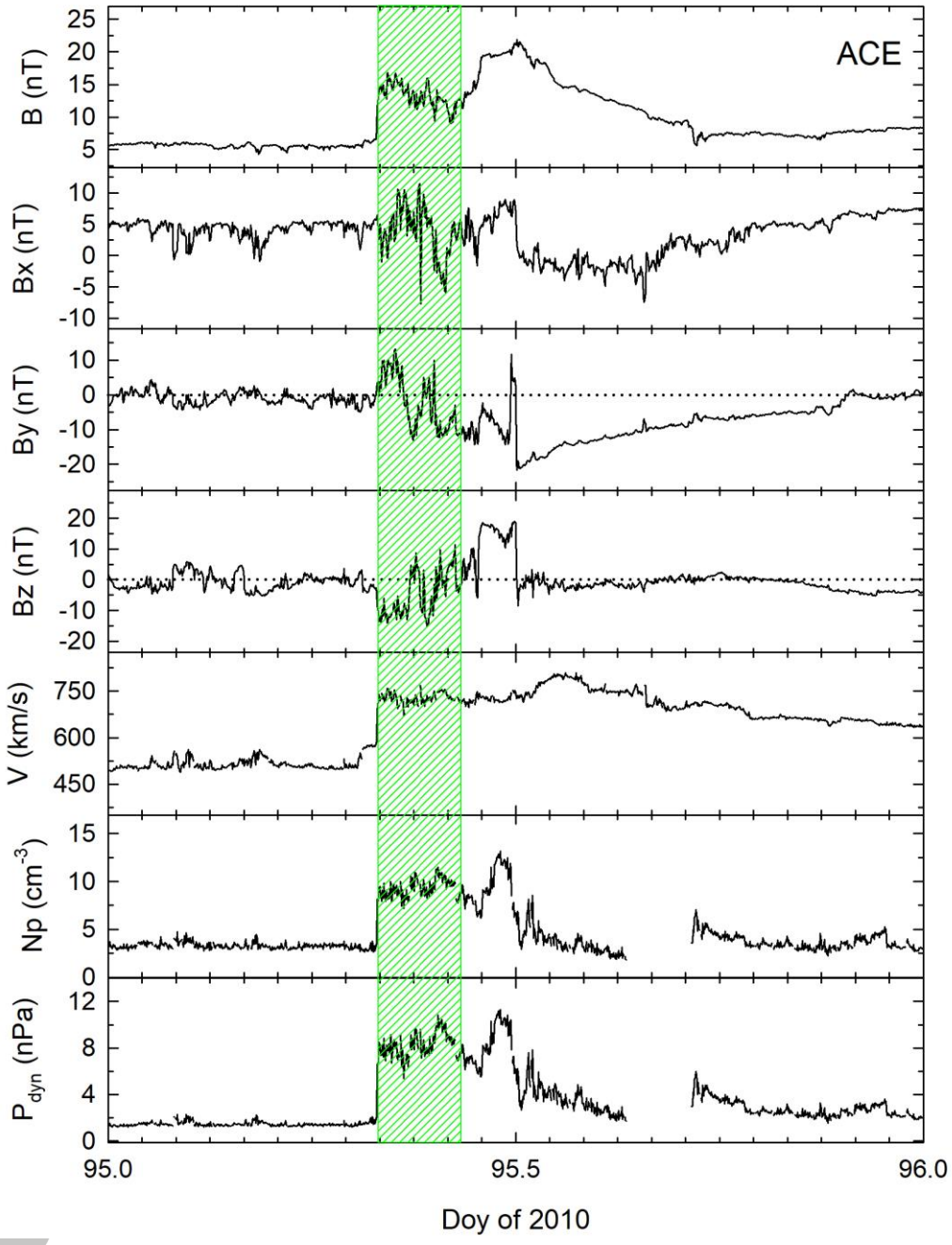

Figure 7. Solar wind parameters from ACE satellite during 5 April of 2010 (Doy 95). From top to bottom, shown is the interplanetary magnetic field strength and IMF GSM components, solar wind speed, proton density and dynamic pressure. The shadowed area corresponds to the interval of increased ionospheric currents above DED and SIT shadowed in Figure 5 shifted 30 minutes ahead by considering data propagation from ACE. Horizontal black dotted lines in Bz and By panels mark the value 0 as reference.

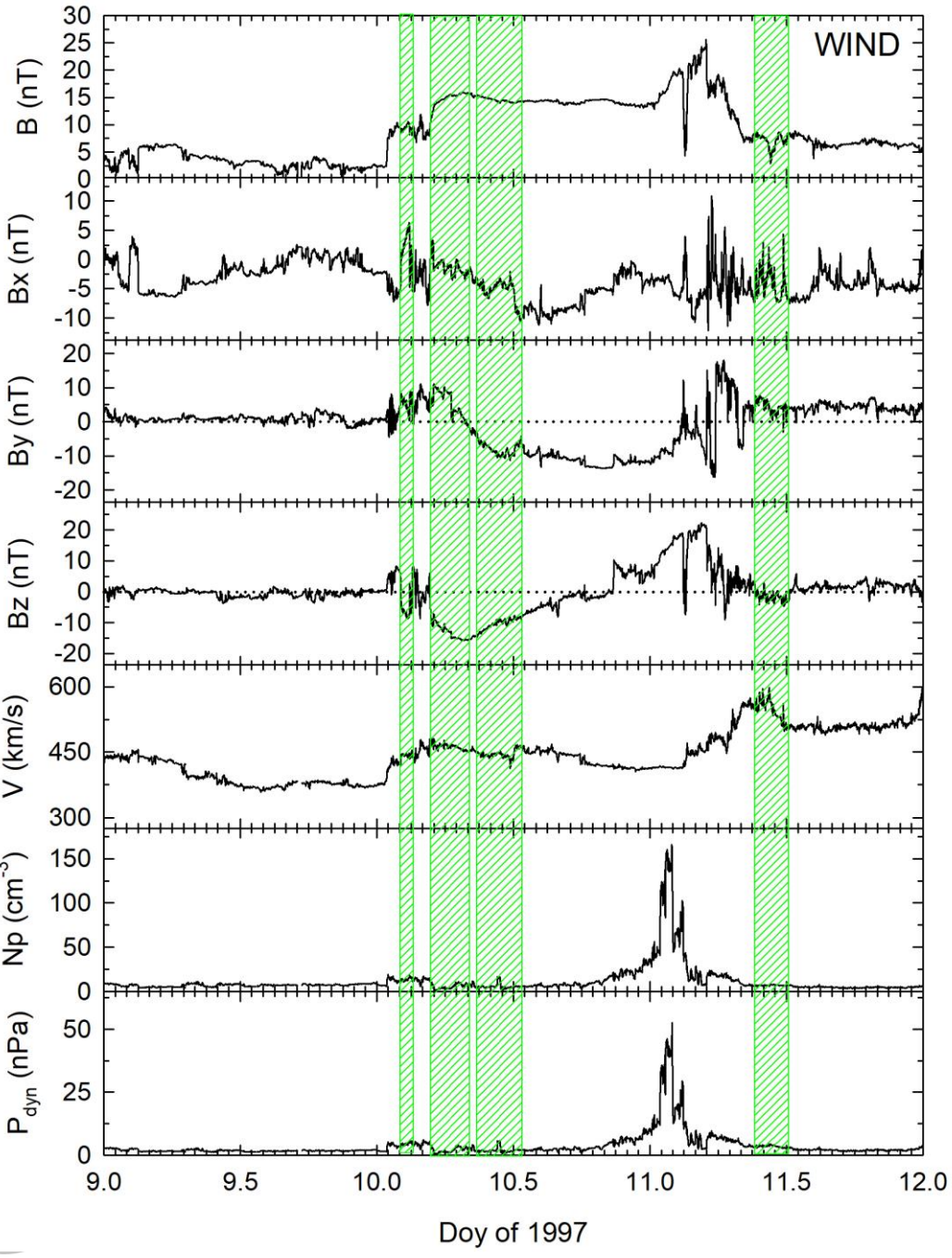

Figure 8. Solar wind and IMF from the Wind satellite during 9-11 January 1997. From top to bottom, shown is the interplanetary magnetic field strength and IMF GSM components, wind flow speed, solar wind density and dynamic pressure. The shadowed areas correspond to the intervals of ionospheric currents increased above BLC and GIM shadowed in Figure 4, 90 minutes ahead by considering solar wind propagation from Wind to the ground. Horizontal black dotted lines in Bz and By panels mark the value 0 as reference.

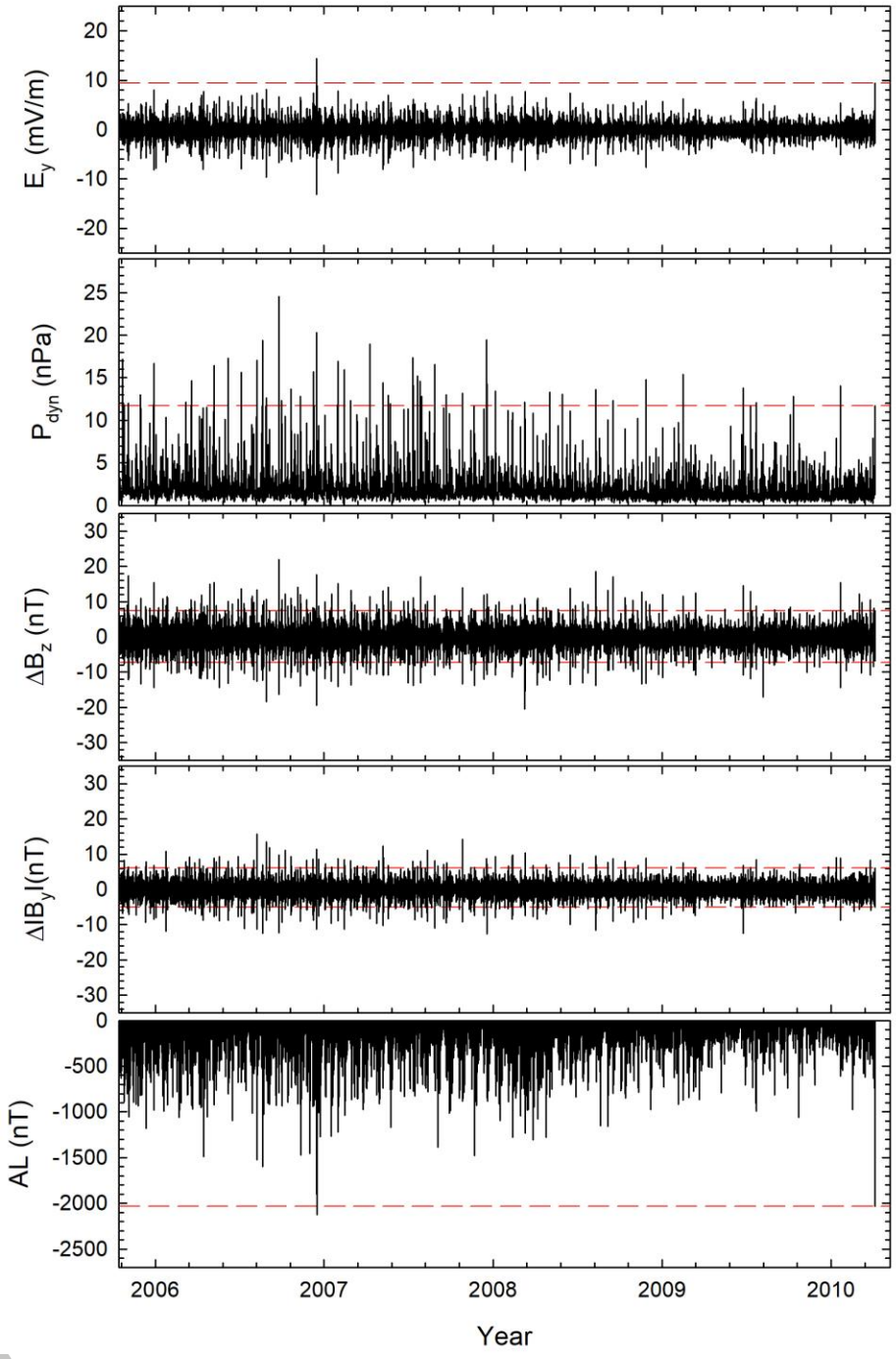

Figure 9. Historical solar wind conditions and AL index from 13 October 2005 (when Galaxy 15 was launched) to 5 April 2010 at 09:50 UT (date of the Galaxy). From top to bottom shown is 5 min dawn-dusk component of interplanetary electric field, dynamic pressure, ΔBz, Δ|By|, as indicative for triggering substorms, and geomagnetic 5 min AL index. The horizontal red dashed lines indicate the maximum values on 5 April 2010.

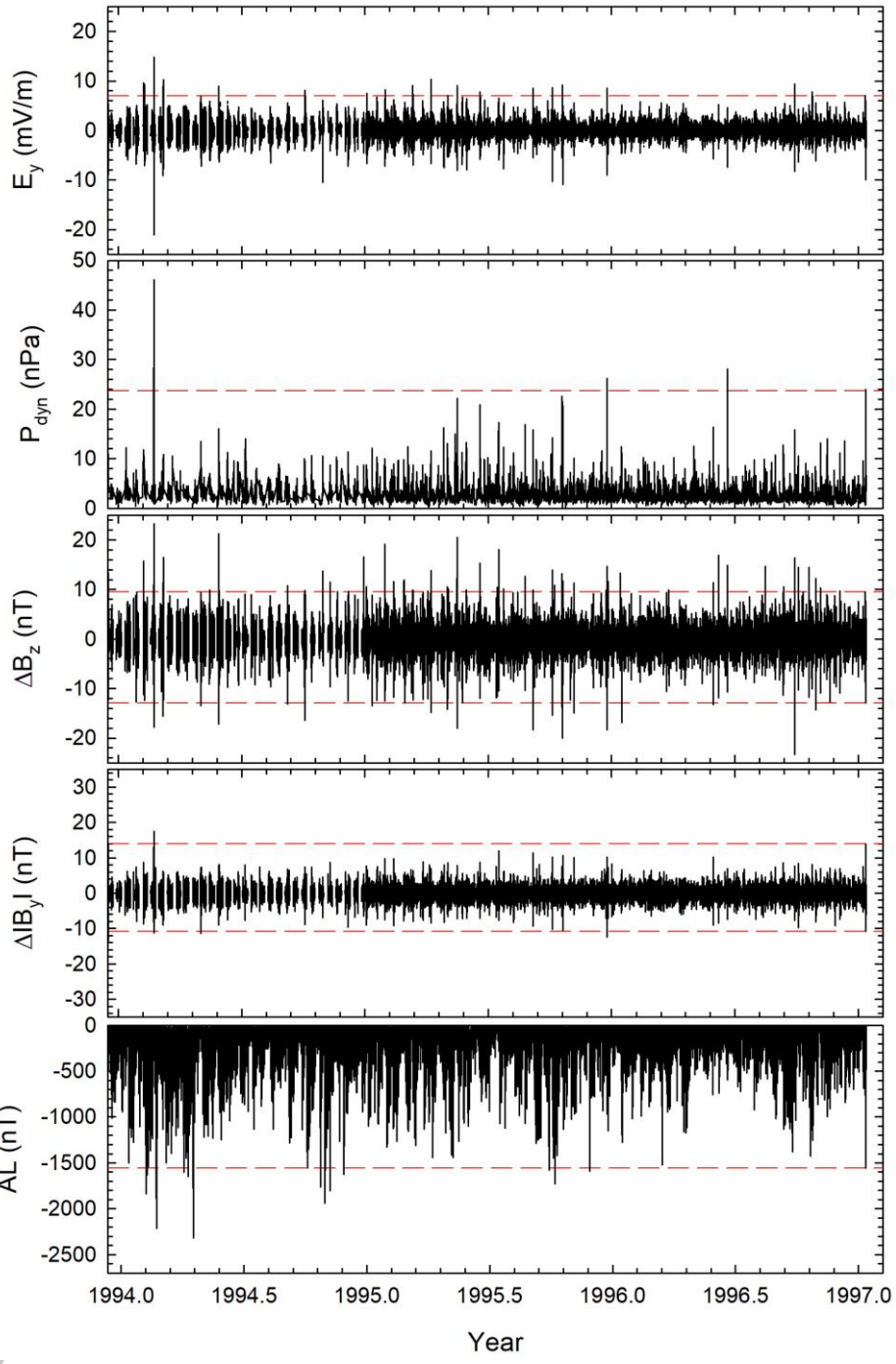

Figure 10. Historical solar wind conditions and AL index from 16 December 1993 (when Telstar 401 was launched) to 11 January 1997 at 11:15 (date of the Telstar 401 anomaly). From top to bottom shown is 5 min dawn-dusk component of interplanetary electric field, dynamic pressure, ΔBz, Δ|By|, as indicative for triggering substorms, and geomagnetic 5 min AL index. The horizontal red dashed lines indicate the maximum values from 10 January 1997 to the anomaly.